Indian Journal of Geo Marine Sciences
Vol. 46 (03), March 2017, pp. 453-461

Anisotropic multi-component seismic identification of gas hydrate in deep water environments of Shenhu area in the South China Sea

Qing Wang [1, 2], Yun Wang [3,4*], Zhiwei Liu[5]& Shiguang Guo[6]

[1]Institute of Geology and Geophysics, Chinese Academy of Sciences, Beijing 100029, China
[2] Key Laboratory of Petroleum Resources Research, Chinese Academy of Sciences, Beijing 100029, China
[3]Institute of Geochemistry, Chinese Academy of Science, Guiyang, Guizhou 550002, China
[4] School of Geophysics and Information Technology, China University of Geosciences (Beijing), Beijing 100083, China
[5]Chinese Academy of Geological Sciences, Beijing 100037, China
[6]ConocoPhillips School of Geology and Geophysics, University of Oklahoma, Norman 73019, USA

*[E-mail: wangqing@mail.iggcas.ac.cn]

Received 20 August 2014; revised 08 April 2015

Gas hydrate bearing zone are significantly affected by anisotropy in Shenhu area, South China Sea. The research takes the changing velocity field of sea water and anisotropic elastic parameters into account to models for simulation. Full-wave field forward simulation data with different saturation of gas hydrate has been generated. Anisotropy field separation method is used to provide more accurate seismic data of pp and ps waves. Study shows that anisotropy has a significant impact on multi-component AVA characteristics, the values of gradient and polarity reversal angle. In addition, multi-component sweetness seismic attribute can be used as significant seismic attribute to identify gas hydrate reservoirs.

[**Keywords:** Anisotropy, Gas hydrates, Multi-component, AVA, Seismic attribute, Anisotropy field separation]

Introduction

Natural gas hydrates has become a major potential mineral resources in the twenty-first century. It is considered to be ideal follow up energy in the future, because per cubic meter ofhydrate can release 164 m^3 of natural gas [1, 2]. However, the release of natural gas hydrates would results in drill accident on the other side[3]. In the worldwide, the current investigation and discovery for natural gas hydrates are inextricably linked with the application of geophysical techniques.The new methods of seismic data processing, interpretation and inversion are constantly used in the study of gas hydrates[4]. The most important methods for identification of gas hydrates include bottom simulation reflector (BSR) and amplitude blank of seismic section. However, it has been found that BSR do not exist in the Blake Ridge, Gulf of Mexico, though these places have found gas hydrates [5]. The same as BSR, amplitude blank highlights technique also has multiple interpretation[6]. Subsequently, amplitude variation with angle of incidence (AVA analysis) and amplitude variation with offset (AVO analysis) were widely used to study gas hydrate reservoir.The AVA or AVO is sensitive to differences in Poisson's ration, when seabed sediments contain gas hydrate, free gas or liquid water[7, 8].

By integrated using these methods, we can better judge whether the deposited layer of gas hydrate and its underlying free gas exists. In addition, some new seismic imaging techniques such as pre-stack depth migration help us figure out its basic distribution9. However, partly due to the lack of shear-wave data, it is difficult to do a further evaluation on distribution of its pore fluid. China has launched the investigations for gas hydrate since 2003 in the South China Sea. Xue Wei Liu (2005) proposed that the profile of P wave to S wave velocity ratio and Poisson's ratio could be used to identify gas hydrate and free gas[9, 10]. Jing Liang (2005) use raytracing method to calculate the interval velocity of seismic profiles A in the North slope of the South China Sea. The study shows that the higher velocity zone in the lower velocity background is an important characteristic of gas

hydrate existing. It also reveals that the high-resolution velocity analysis is useful not only to search the hydrate spot but also to estimate the rich layer of gas hydrate[11, 12].

With the utilization of OBC/OBS (Ocean Bottom Cable/Ocean Bottom Seismometer) multi-component seismicacquisition system in Shenhu area of the South China Sea, more information includes converted PS wave would be used to analyse characteristics of gas hydrates. However, at present, researches about gas hydrates in Shenhu area by multi- component wave has been in use considering anisotropic gas hydrates behaviour in Shenhu area is in preliminary stage. In addition, the average depth of sea water inShenhu study area is over 1000 meters[13]. The impact of the deep water environment on seismic amplitude, phase and travel time is significant. Because velocity varies with water depth, there is a difference of seismic traveltime, ray paths, and amplitude, which affect the migration imaging results if sea water propagation velocity is still taken as constant for the propagation wavefield[14].To solve these problems, we calculate the velocity field of deep water in the study area by physical and chemicalproperties of sea water. Through analysis of core data from study area, elastic parameters of sediment and anisotropy parameters in different saturation of gas hydrate reservoirs are determined. Using these parameters, we have established a set of models of elastic anisotropy and forward full-wave fieldsimulation data. Moreover, P-wave and PS-wave on each component is accurately separated by advanced wave field separation techniques. On the basis of these data, some anisotropic AVA/AVO characteristics and new multi-component seismic attribute are obtained and usedto guide analysis of the coming field OBC/OBS seismic data.

Materials and Methods

Geological background:

The study area is a passive margin. Its structure is located in the Pearl River Mouth Basinof the northern South China Sea.The depth of water in this region is 200~2000 meters, depression area is 20000 km^2.Thickness of Cenozoic sediment is more than 1000 m. The study area has the largest depression area and the thickest sediment in the Pearl River Mouth Basin. In Cenozoic Era, the research area has gone through three phases of tectonic evolution: riftting stage, thermal subsidence and neotectonic stage. In the rifting stage, the prototype of the sag was formed by faulting in seabed and filled with deltaic-lacustrine-fan deltaic depositional systems8, 9(Fig.1).

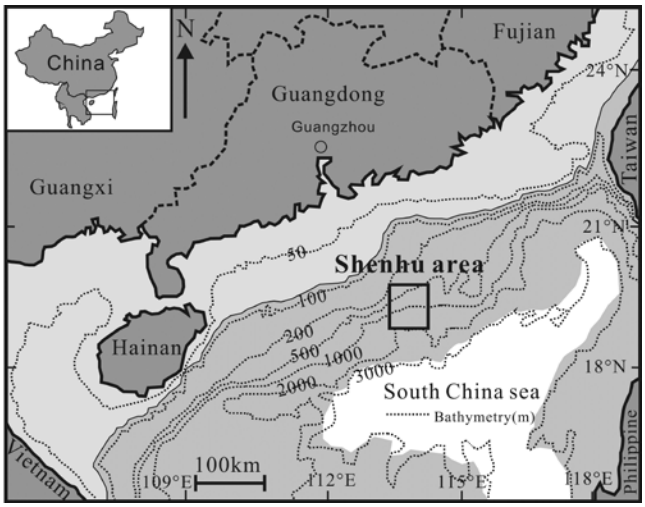

Fig. 1-Schematic diagram of the location and topography of the Shenhu area: black box shows the study area

Due to the control of faults in the Northeast and Northwest, seabed topography progressively stepped down in the northern South China Sea. Geological landforms, submarine plateau, mesa slope, erosion trenches, undersea cliffs, steep slopes and sea submarine valley are developed in the slope[15]. These faults cut through some relatively sedimentary layer and extend to near the seafloor. These geological movements create favourable conditions for gas hydrate migration to shallow stability zone. The widely distributed gas chimneies are considered as the significant gas transportation. In addition, the fold structure is easy to capture natural gas, prompting the formation of gas hydrates in the study area[16].

Model of velocity and density of deep water:

In the deep water environment, sea water exist stable stratification. Acoustic wave propagation in the sea water exhibits nonlinear characteristics with the change in the depth. Currents and the small-scale processes also results in disturbance of acoustic wave in propagation[17]. These effects will lead to anisotropic behaviour in the velocity field. They can also result in the loss of seismic energy and changes of amplitude and phase. The acoustic velocity of sea water varies with depth, pressure, salinity and temperature. It cannot take as a constant value 1500 m/s. Therefore, when simulating the speed of sound in sea water, we use the famous MacKenzie equation:

$$V(D,S,T) = 1448.96 + 4.591T - 5.304\times10^{-2}T^2 + 2.374\times10^{-4}T^3 + 1.340(S-35) + 1.630\times10^{-2}D + 1.675\times10^{-7}D^2 - 1.025\times10^{-2}T(S-35) - 7.139\times10^{-13}TD^3 \quad (1)$$

Where T, D, S, V are temperature (Celsius), depth (meters), salinity (‰ppt), and velocity (m/s) respectively. Using the CTD (Conductance, Temperature, Salinity and Depth) data and MacKenzie equation, we calculate the exact velocity of sea water. Moreover, the UNESCO (United Nations Educational, Scientific and Cultural Organization) sea water equation is used to obtain the density and pressure of sea water[17]. Fig.2 shows the elastic model of sea water.

Drilling data shows the average thickness of gas hydrate is 300 meters. In the upper sedimentary, average thickness of shallow sedimentary is 500 meters. Free gas exists underneath the gas hydrate zone. Sedimentary bedrock is below free gas. Fig. 4 displays the schematic diagram of velocity model. The average depth of sea water is 1000 meters. The velocity and density of sea water are from the model data above. Velocity and density of shallow sediment is increasing with depth and obtained by drilling data[19]. The most important elastic parameters of gas hydrate are shown in Table 1. In Table 1, gas hydrate with different saturation has different elastic parameters.

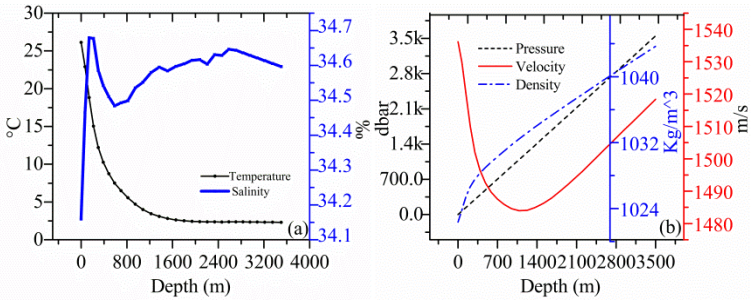

Fig. 2-Temperature, salinity (a) and velocity, density and pressure (b) with the depth of sea water in research Shenhu area

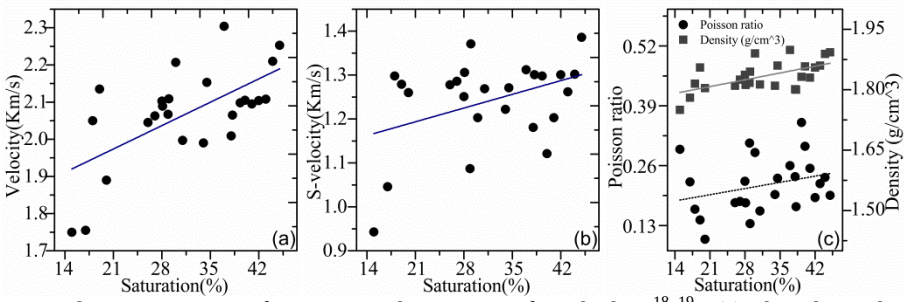

Fig. 3-Relationships between elastic parameters of reservoir and saturation of gas hydrate[18, 19]: (a) The relationship between P-velocity and saturation of gas hydrate: Vp =1785.18+898.41*s; (b) The relationship between S-velocity and saturation of gas hydrate: Vps =1099.85+446.49*s ;(c) The relationship between density and saturation of gas hydrate: ρ =1757.02+241.42*s

Anisotropic elastic parameters of reservoir:

Through information of drilling and core data, elastic and anisotropic parameters of the study area are obtained[18]. Fig. 3(a) and (b) shows the relationship between the saturation of gas hydrate and velocity of P, S wave respectively. We get the mathematical relationship between the velocity of P, S wave and saturation of gas hydrate by least squares fitting. Fig. 3 (C) shows the relationship between the density and saturation hydrate of gas hydrate, and the fitting mathematical relationships.

The average velocity of P-wave and S-wave linearly increases with the increase of the saturation. Meanwhile, gas hydrate density also increases as the velocity of wave increases.

In terms of anisotropy parameters, shallow sedimentary seabed δ is 0.01; ε is 0.01; gas hydrate δ is 0.1; ε is 0.09; underlying free gas δ is 0.003; ε is 0.001. Air gun is used to stimulate during the simulation, while seismic signal is received by submarine OBC system. Set the receiver channel number at 100, the dominant frequencyis 60Hz Ricker wavelet.

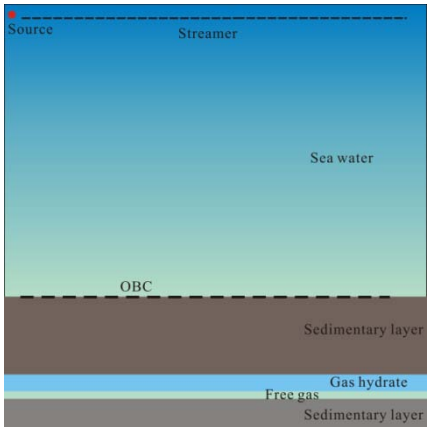

Fig. 4-Schematic diagram of model

Method of wave field separation:

When three-component geophones are used in the multi-waves seismic exploration, Z component can not only record the P wave but also record S wave in perpendicular to the surface. Similarly, X component not only record S wave component, but also has recorded a partial component of the P wave. In anisotropic conditions, wave fields interfere with each other more serious[20]. For inhomogeneous anisotropic VTI media, the polarization direction of P and S wave be solved by the Christoffel equation, then we use inverse Fourier transform to get the separation operator of wave field in spatial domain. Finally achieve wave field separation in inhomogeneous anisotropic medium.

In the actual exploration and experimental tests, it was found that existing rocks in the earth crust shows anisotropic characteristic problems. Anisotropic media refers to the change of physical nature in the various directions. According to the stress continuity condition and displacement between two sides of the interface, Daley and Hron (1977) deduced the precise formula of the reflection and transmission coefficients[21]. Banik (1987) explained its physical significance. He also deduced approximation formulas derived from Delay and Hron's (1977) coefficients formula by Thomsen anisotropic parameters[22]. When incident wave is P wave, the following relationship was derived:

$$R_{APP}(\theta) = R_{IPP}(\theta) + \Delta\delta / 2 * \sin^2\theta \quad (2)$$

Where $R_{IPP}(\theta)$ is reflection coefficient in isotropic medium; $R_{APP}(\theta)$ is reflection coefficient in anisotropic medium. $\Delta\delta = \delta 2 - \delta 1$ (δ2 and δ1 is values above and below the interface respectively).

In VTI anisotropic media, PetrJilek and Vavrycuk (1998) provides approximate formula for Ps wave reflection coefficient formula. This formula includes Thomsen anisotropic parameters, angle of incidence and incidence azimuth function[23]. In order to ensure the accuracy of the approximate formula, we use its third order approximation formula:

$$R_{PSV}^{VTI}(\theta) = A\sin\theta + B\sin^3\theta \quad (3)$$

Parameters A and B are shown in Table 2.

Anisotropic AVO analysis:

Table 1— Elastic parameters of gas hydrate

Attributes	1	2	3	4	5
Saturation (*%*)	15	22	29	36	42
P-velocity(*m/s*)	1919.9	1982.8	2045.7	2108.6	2162.5
S-velocity(*m/s*)	1166.8	1198.1	1229.3	1260.6	1287.4
Poisson ration(μ)	0.2071	0.2125	0.2174	0.2219	0.2255
Density(ρ)	1793.2	1810.1	1827	1843.9	1858.4

Table 2-Parameters expression

Coefficient	Isotropic background	Anisotropic disturbance
A	$-(1/2+\kappa)*\Delta\rho/\rho_{av}-2\kappa*\Delta\beta/\beta_{av}$	$(1/2(1+\kappa))*(\delta_2-\delta_1)$
B	$(3/4*\kappa^2+1/2*\kappa)*\Delta\rho/\rho_{av}+$ $(2\kappa^2+\kappa)*\Delta\beta/\beta_{av}$	$1/(1+\kappa)*(\varepsilon_2-\varepsilon_1)+$ $((\kappa-4)/4(1+\kappa))*(\delta_2-\delta_1)$

Notes: Density $\Delta\rho=\rho_2-\rho_1$; $\rho_{av}=(\rho_2+\rho_1)/2$; velocity of P wave is a, $a_{av}=(a_2-a_1)/2$; velocity of S wave is β, $\beta_{av}=(\beta_2-\beta_1)/2$, $\kappa=\beta_{av}/a_{av}$. $\Delta\delta=\delta_2-\delta_1$, $\Delta\varepsilon=\varepsilon_2-\varepsilon_1$. Parameters δ and ε are Thomsen anisotropic parameters.

Results and Discussion

Vertical component (Z) and horizontal component(X) which is obtained from the simulation are shown in Fig.5 (a) and Fig. 6(a) respectively. Fig.5 (b) shows the data of Z component after separation. Fig. 5(c) is the enlarged display of the white box in Fig. 5 (a). The red box illustrates S interference wave in Z component. By adopting anisotropic wavefield separation, a part of S wave in vertical (Z) component is suppressed (Fig.5 (d)). As

well as Z component, horizontal component (X) also records a little P wave (Fig.6 (c)). Using the method of anisotropic wavefield separation, the interference P wave in X component is suppressed (Fig.6 (b), (d)).

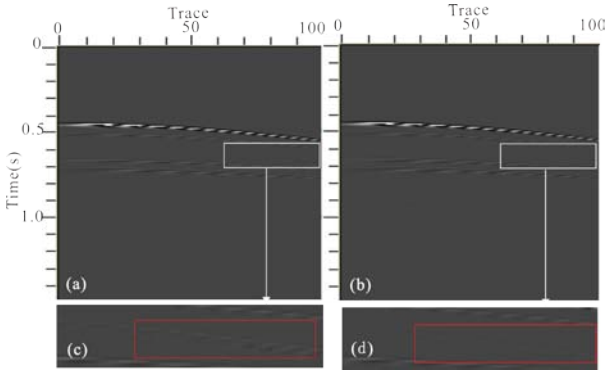

Fig.5-Anisotropic wavefield separation in Z component (a) The original data of Z component; (b) The data of Z component after separation; (c) Enlarged display of the white box in (a); (d) Enlarged display of the white box in (b);

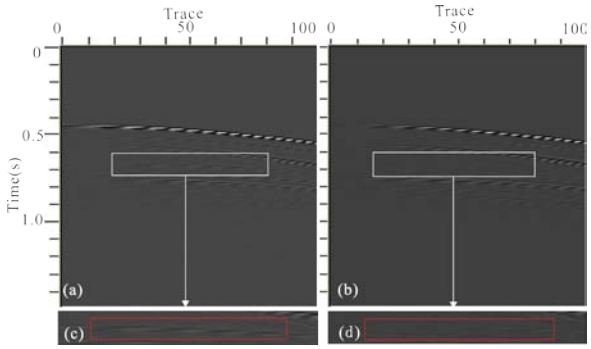

Fig.6-Anisotropic wavefield separation in X component: (a) The original data of X component; (b) The data of X component after separation; (c) Enlarged display of the white box of (a); (d) Enlarged display of the white box of (b)

In the isotropic medium, the P wave reflection coefficient (Rpp) decreases with the increase of the gas hydrate saturation. Fig.7 (a) demonstrates that gas hydrate with 42% saturation has the minimum Rpp. As the incident angle increases, the absolute values of Rpp also increase, the sign is negative. As the angle of incidence continues to increase, Rpp with 42% saturation is the first one to reaches a maximum value and begins to change the direction. Rpp with 15% saturation is the last one.For the converted wave, however, the PS wave reflection coefficient (Rps) increases with the increase of the gas hydrate saturation (Fig.7 (b)). The bigger the saturation is, the bigger the gradient of Rps. As the incident angle increases, the absolute values of Rps increase. Rps with 42% saturation is the last one to reaches a maximum value and begins to change the direction. Rps with 15% saturation is the first one.We can see this phenomenon from the black arrow in Fig.7 (b). In the background of anisotropic medium, the changing trends of the anisotropicreflection coefficient (Rapp) with changing saturation and incident angle stay almost the same trend as Rppin isotropic medium.

With the increasing incident angle, the effect of anisotropic on the P wave reflection coefficient is growing (Fig.8 (a), Fig.9 (a)). Fig.9 (a) shows the difference between Rapp and Rpp. For converted S wave, it can be seen in Fig. 8 (b) that the curves of Raps have no cross with the increase of the incident angle.The difference between Raps and Rps is growing, when the incident angle is less than 28 degree. As the incidence angle continues to increase, the difference between Raps and Rps first reduced to zero, and then increases to a maximum value (Fig.9 (b)).

In the background of isotropic elastic parameters, P wave reflection coefficient (Rpp) of free gas increases with the increase of the gas hydrate saturation. Fig.10 (a) demonstrates that gas hydrate with 42% saturation has the maximum Rpp.However, Rpp of free gas decreases with the increase of incident angle. When the incidence angle continues to increase more than 40 degree, Rpp begins to increase. For the converted S wave, Fig. 10(b) shows that the PS wave reflection coefficients (Rps) of free gas always increase when the incident angle is less than 40 degree.

In the background of anisotropic elastic parameters,the changing trends of Rpp and Rps with changing saturation and incident angle stay the same as them in isotropic medium.With the increasing incident angle, the effect of anisotropic on the P wave reflection coefficient is growing (Fig. 11(a), Fig. 12 (a)). Fig. 11(b) shows that anisotropic expands the Rps span between 42% and 15% saturation. When the incident angle is less than 30°, the anisotropy has low impact on Rps. When the incident angle continues to increase, the impact caused by anisotropy increases rapidly (Fig. 12 (b)).

Sweetness attribute is put forward by Radovich and Oliveros in the late 1990s[24, 25]. It is applied in identification of sand body in clastic. Goff (2004) analyses how to use sweetness attribute to calculate thickness of deepwater turbidite deposit unit. Mathematically, sweetness attribute is the RMS ratio of reflected intensity to instantaneous frequency[26]. Because the physical properties of gas hydrates and clastic sand are very different, the value of sweetness attribute in the sand body would show a high value, but it is hard to obvious in the gas hydrate.Through

analysing of separated multi-component seismic data, we found that the sweetness attribute can be a good seismic attribute to identify gas hydrate reservoirs. Fig. 13 (a) shows a profile of the sweetness attribute. Fig. 13 (b) shows the corresponding values of sweetness attribute in P reflection wave. Arrows show the values of P reflection waves from seafloor and gas hydrate reservoir. We found that there are different on the order of magnitude of these data between seafloor and gas hydrate reservoir. Calculations of data display that values of sweetness seismic attribute increase in P wave and have almost no change in S wave, with the increasing degree of saturation of gas hydrate reservoir. The ratio of sweetness attribute of P wave to its in S wave decreases with the increasing of saturation. The magnitude of gradient is equalization (Fig.14).

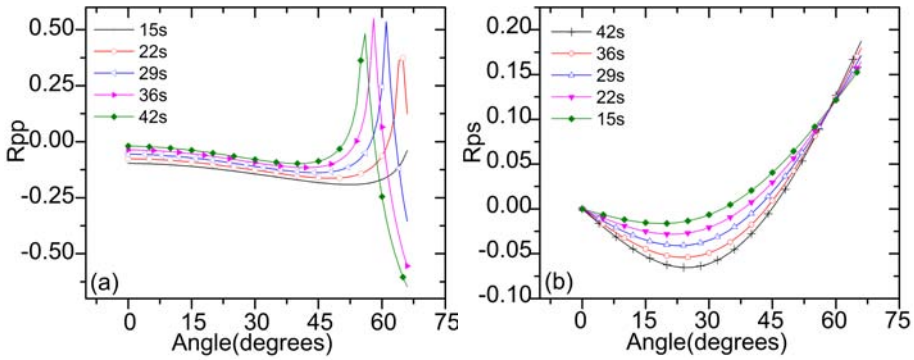

Fig.7-P reflection coefficients (a) and S reflection coefficients (b) of gas hydrate vs incident angle in isotropic background

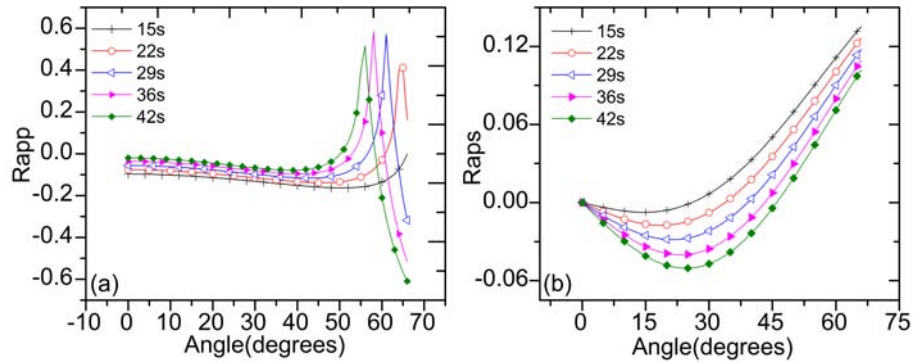

Fig.8-P reflection coefficients (a) and S reflection coefficients (b) of gas hydrate vs incident angle in anisotropic background

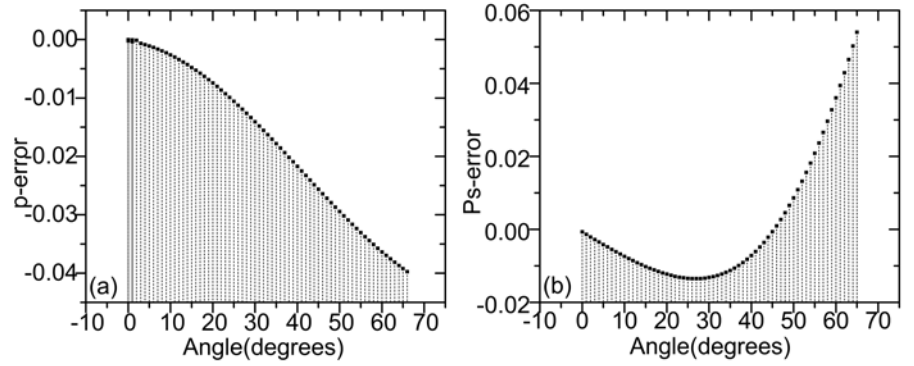

Fig.9-Average differences between Fig. 7 and Fig. 8

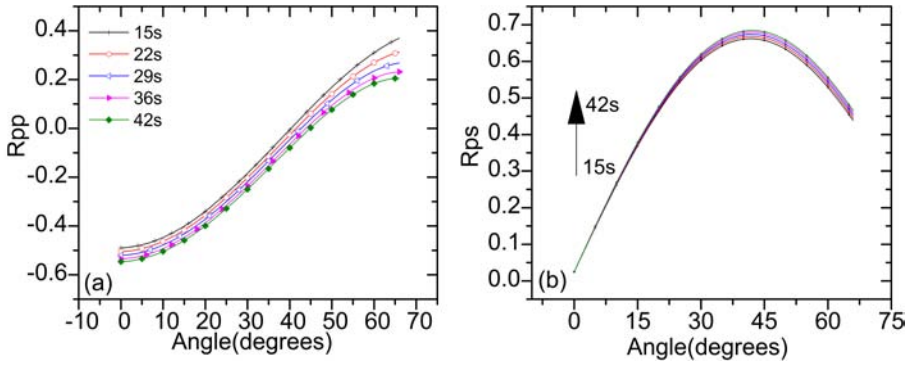

Fig.10-P reflection coefficients (a) and S reflection coefficients (b) of free gas vs incident angle in isotropic background

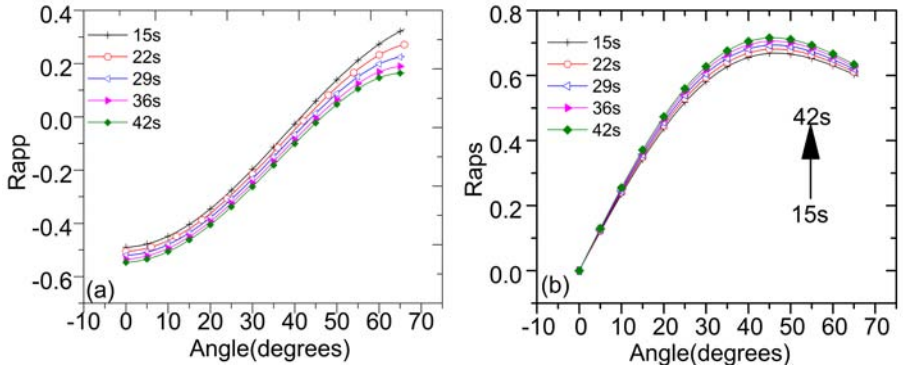

Fig.11-P and S reflection coefficients (a) and S reflection coefficients (b) of free gas vs incident angle in anisotropic background;

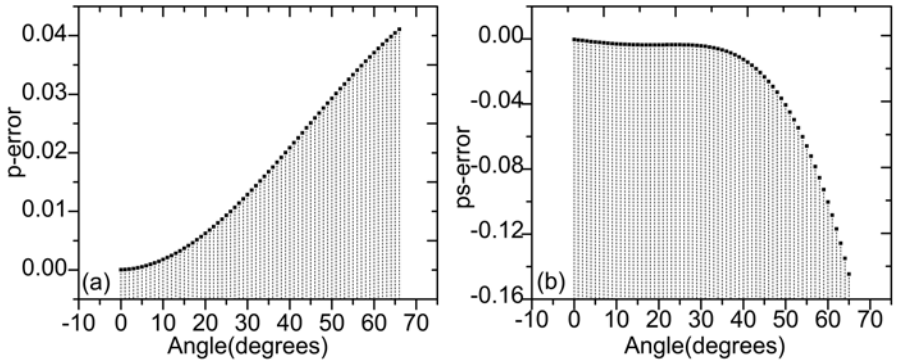

Fig. 12-Average differences between Fig. 10 and Fig. 11

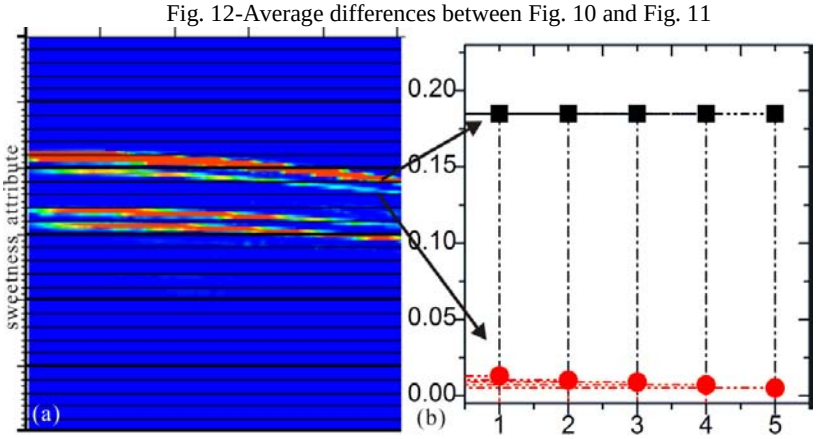

Fig. 13-Sweetness attribute profile and schematic diagram

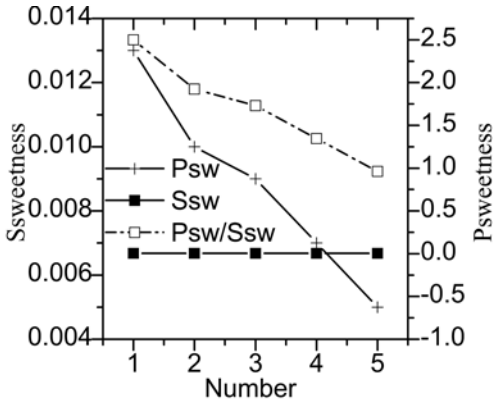

Fig.14-Sweetness attribute profile and schematic diagram

Conclusion

The study takes into account changing velocity field of sea water, anisotropic elasticparameters and saturation of gas hydrate to forward modelling.

Result shows that we can combine the AVA and anisotropic AVA features of Pp and Ps wave to identify the different saturation (from 15% to 45%) gas hydrate and free gas. Anisotropy has a greater impact on AVA of Ps wave than Pp wave. 28 and 30 degree incidence angle is the point mutations of anisotropy affecting AVA of Ps wave for gas hydrate and free gas respectively. Using multi-wave sweetness seismic attribute, gas hydrate with different saturation can identify from turbidite deposit unit.

Acknowledgement

Project supported by the National Science and Technology Major Project of the Ministry of Science and Technology of China (GrantNo.2011ZX05035-001-006H,2011ZX05008-006-22,2011ZX05049-01-02,2011ZX05019-003).The research and development of "elastic wave seismic imaging technology" by China National Petroleum corporation. The project of "10 dimensional 3D predictions and connectivity of the fractured vuggy in Tahe, China" also give support.

References

1 Andreassen, K., Hart P.E. and Mackay, M., Amplitude versus offset modeling of the bottom simulating reflection associated with submarine gas hydrates. *Mar. Geol*, 137(1997): 25-40.

2 Max, M.D. and Lowrie, A.,Oceanic methane hydrates: A “frontier” gas resources. *J. Petrol. Geol.*, 19(1996) 41-56.

3 Liang, J., Wang, M.J. and Wang, H.B., Relationship between the sonic logging velocity and saturation for gas hydrate in Shenhu area, northern slope of South China Sea. *Geosci.*, 23(2009) : 217-223.

4 Carolyn L, Song, G.Q., Cong, L.Z.and Mu, X., Fault control on hydrocarbon migration and accumulation in the Tertiary Dongying depression, Bohai Basin, China. *AAPG Bull.,* 99(2012): 983-1000.

5 Carcione, J. M. and Tinivella,U., Bottom-simulating reflectors: seismic velocities and AVO effects. *Geophysics*, 65(2000): 54-67.

6 Shankar, U. and Sain, K., Heat flow variation from bottom simulating reflector in the Kerala-Konkan basin of the western continental margin of India. *Indian J. Mar.Sci.*, 38 (2009): 110-115.

7 Sarmadi, D., Hashemi,M. H. and Sokooti, R., AVO analysis for Gas Hydrate Bearing Zone of Oman Sea, paperpresented at the International Geophysical Conference and Oil & Gas Exhibition, Istanbul, Turkey, 2012.

8 Zhang,Z.J.,Daniel,R.,McConnell.andHan .H.,AVOcrossplot analysis in unconsolidated sediments containing gas hydrate and free gas: Green Canyon 955, Gulf of Mexico,paper presented at the SEG International Exposition and 82th Annual Meeting, Las Vegas, USA,2012.

9 Ramadlona, V. and Chen, H.W., Simultaneous imaging of BSR for methane hydrate exploration and ocean current fine structures,paper presented at the SEG International Exposition and 84th Annual Meeting, Denver, USA,2014.

10 Liu, X.W., Li, M. F. and ZHANG, Y.W., Studies of seismic characteristics about gas hydrate: A case study of line.HD152 in the South China Sea. *Geosci.*, 19(2005): 33-38.

11 Liang, J., Wang, H.B. and Zhao, Z.C., The application of ray tracing method in velocity analysis of gas hydrate of the South China Sea. *Comp.Tech.Geophys.Geochem.Exp.*, 29(2007): 486-491.

12 Shankar, U. and Michael, R., Gas hydrate saturation in the Krishna–Godavari basin from P-wave velocity and electrical resistivity logs. *Mar.Petrol.Geol*., 28(2011) 1768-1778.

13 Lu, J.A., Yang, S.X.and Wu,N.Y.,Well logging evaluation of gas hydrates in Shenhu area, South China Sea., *Geosci.*, 22(2008): 447-451.

14 Bertrand,A. and Macbeth,C., Seawater velocity variations and real time reservoir monitoring. *T.L.D.,* 22(2003): 351-355.

15 Sun, Y. B., Wu, S.G., Dong, D. and Gong,Y.H., Gas hydrates associated with gas chimneys in fine-grained sediments of the northern South China Sea. *Mar.Petrol.Geol*.,311(2012): 32-40.

16. Wu, N.Y., Zhang, H.Q. and Zhang, G.X., Gas hydrate system of Shenhu area, northern South China Sea: geochemical results, *J.Geol.Res*. 3(2011): 1-10.

17 Han, F.X., Sun, J.G. and Wang, K., The influence of sea water velocity variation on seismic traveltimes, ray paths, and amplitude. *App. Geophys*.9 (2012): 319-325.

18 Deng, G., Deepwater gas hydrate investigatoin report, Shenhu survey area, South China Sea, offshore China, Report, Guangzhou Marine Geological Survey. Guangzhou, China, 2007.

19 Li, G., Li, X.S. and Chen, Z.Y., Numerical simulation of gas production from gas hydrate zone in Shenhu area, South China Sea. *Acta.Chim.Sinica*., 11(2010): 1083-1092.

20 Sun, R., Mcmechan, G. A. and Chuang, H.H., Amplitude balancing in separating P and S waves in 2D and 3D elastic seismic data. *Geophysics*, 76(2011): 103-113.

21 Dely, P.F. and Hron, F.,Reflection and transmission coefficients for transversely isotropic media. *Bull.Seis. Soc. Am*., 67(1977): 661-675.

22 Banik,N.C., An effective anisotropy parameter in transversely isotropic media. *Geophysics*, 52(1987): 1654-1664.

23 PetrJilek,I. and Vavrycuk,V.,Weak contrast PP wave displacement R/T coefficients in weakly anisotropic elastic media. *Pure.Appl.Geophys.*, 151(1998): 699-718.

24 Shoar, B.H., Javaherian, A.,Farajkhah, N.K. and Arabani, M.S., Reflectivity template, a quantative intercept gradient AVO analysis to study gas hydrate resource-A case study of Iranian deep sea sediments. *Mar. Petrol.Geol*.,51(2014): 184-196.

25 William, J.W., Ingo.,A.P.,Willian, F.W. and David,H.M., Physical properties and rock physics models of sediment containing natural and laboratory formed methane gas hydrate. *Am.Mineral*., 89(2004): 1221-1227.

26 Goff, D., Estimating net: gross from datahistograms: Examples from deep-water turbidites, Report, the regional West Africa business Chevron,TX, USA.